

High fidelity quantum gates via analytically solvable pulses

Sophia E. Economou

Naval Research Laboratory, Washington, DC 20375, USA

(Dated: March 3, 2013)

It is shown that a family of analytically solvable pulses can be used to obtain high fidelity quantum phase gates with surprising robustness against imperfections in the system or pulse parameters. Phase gates are important because they can implement the necessary operations for universal quantum computing. They are particularly suited for systems such as self-assembled quantum dots, trapped ions, and defects in solids, as these are typically manipulated by the transient excitation of a state outside the qubit subspace.

The physical implementation of quantum computation requires high quality coherent gates. Single qubit rotations combined with the conditional C-Z phase gate form a universal set of quantum logic gates [1]. Time dependent controls, such as lasers, are used in order to implement these prescribed unitary evolutions of the qubits.

In many physical systems, such as self-assembled quantum dots [2–5] and quantum wells [6], trapped ions [7] and atoms [8], defects in solids [9], and in some cases superconducting qubits [10], auxiliary states outside the Hilbert space of the qubit are used in order to implement these gates. One advantage of using such states is that their energy splitting from the qubit states is typically orders of magnitude larger than the qubit splitting itself and thus fast operations can be achieved, since the time scales as the inverse of the energy. For unitary evolution within the qubit space, these excited states should be only transiently excited, and fast operations are key in order to avoid incoherent decay back to the qubit states.

The most familiar gate is the induction of a minus sign in front of one of the qubit states via cyclic resonant excitation of the excited state. As shown in Fig. 1, the two qubit states $|n\rangle$ and $|\bar{n}\rangle$ (which can be thought of as spin eigenstates along the \mathbf{n} direction, or as a subset of two-qubit states) are respectively coupled and uncoupled from the excited state by a pulse. A path that excites the population in state $|n\rangle$ resonantly to $|E\rangle$ and returns it through a cyclic evolution will induce a minus sign to state $|n\rangle$. This is a familiar property of quantum systems that differentiates (pseudo)spin from spatial rotations in euclidian space, where a full 2π rotation returns the system to its starting point.

Indeed, this evolution has been used in the demonstration of quantum gates of a variety of systems, including semiconductor nanostructures [3, 6, 11, 12], trapped ions [13] and fullerene molecules [14]. This is done straightforwardly by a resonant pulse of any temporal profile. In contrast, the implementation of other phase gates is non trivial, since the majority of pulses will leave the system partially in the leaky excited state $|E\rangle$. Perturbative methods such as adiabatic elimination [15] of state $|E\rangle$ partially address this, but they have the inherent drawback of a need for long pulses. Exact analytically solvable dynamics are therefore highly desirable, since they can

guarantee that the probability of the population remaining in the excited state is zero after the passage of the pulse. Moreover, they provide a reliable recipe for tuning parameters to achieve the target evolution. In that spirit, the well-known hyperbolic secant (sech) pulse [16] was proposed [17] and later used experimentally for the demonstration of electron [3] and exciton [12] spin rotations in quantum dots.

While the sech pulses considered in [3, 12, 17] have been successful for the experimental demonstration of spin gates, they do not yield the near perfect fidelities needed for quantum computing. The main shortcomings of these pulses are the (near) resonant excitation of the lossy excited state required to achieve large phases and the sensitivity of the induced phase to small variations in the detuning. As a result, an experimental error in the laser frequency induces errors in phase, while in an ensemble of systems with unequal energy splittings this can lead to dephasing in the net signal [3].

In this work, these issues are addressed by use of a family of pulses that generally feature asymmetric profiles and frequency modulation (‘chirp’). Focusing on cyclic evolutions by two different pulse strengths, I show that impressive fidelities are obtained by the stronger pulses, which furthermore demonstrate robustness against errors in the parameters. The chirped pulses generally allow for higher fidelities as compared to their unchirped counterparts, an effect reminiscent of the robust population transfer to an excited state using chirped lasers, which has been recently used to that end in quantum dot systems [18, 19]. In the context of the latter experiments, the present work is particularly timely and compatible with state of the art capabilities.

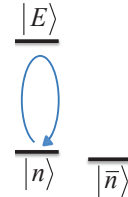


FIG. 1: (Color online) Qubit states ($|n\rangle, |\bar{n}\rangle$) and the auxiliary excited state $|E\rangle$. States $|n\rangle$ and $|E\rangle$ have energy separation ω_{En} and are coupled by a field of frequency ω .

The hyperbolic secant (sech) pulse shape was first discovered by Rosen and Zener (RZ) as a nontrivial driving term that yields an analytically solvable Schrodinger equation of a two-level system. In the 70s the sech pulse gained intense interest in the context of self induced transparency, i.e., as the pulse that does not lose its shape as it propagates through a nonresonant medium [20]. In the 80s a number of papers introduced pulses that also result in analytically solvable dynamics and which are generalizations of the sech, generally containing asymmetry and/or chirping [21, 22]. It was found [21] that asymmetric pulses do not return the population to the ground state, while the same is true for ones with only chirping. However, the combination of chirp and asymmetry allows for cyclic evolution when the chirp and asymmetry parameters are related in a certain way [22].

To solve the time-dependent Schrödinger equation for a coupling with a hyperbolic secant temporal shape $f(t) = \Omega \text{sech}(\sigma t) e^{i\omega t} + cc$, RZ define a new variable $z(t) = 1/2(1 + \tanh(\sigma t))$. In terms of z , they show that the second order differential equation for the probability amplitude of state $|n\rangle$ is the hypergeometric equation, for which the solutions are known. From the solution, one can see that when $\Omega/\sigma = \text{integer}$, the evolution is cyclic, independently of the detuning $\Delta = \omega_{En} - \omega$ from the transition $|n\rangle \rightarrow |E\rangle$.

In the more general case of temporally asymmetric and frequency modulated pulses with envelope $f(t) = 2\sqrt{z(1-z)/(\lambda z + 1)}$ and oscillatory term $e^{i(\omega t + g(t))}$, where $\dot{g} = \beta \frac{(2+\lambda)z-1}{\lambda z+1}$, a similar transformation $t = \sigma^{-1}/2 \ln[z/(1-z)^{1+\lambda}]$ with $\lambda > -1$ puts the equation in a Hypergeometric form. Therefore, the dynamics are analytically solvable, and what changes relative to the RZ solution are the parameters appearing in the Hypergeometric functions, which are now functions of not only the pulse strength and frequency, but also the asymmetry and the chirp. In this general case, the probability of return does depend on the detuning as well in the following way: when the chirp parameter β is related to the asymmetry via $\beta = -\lambda\Delta/(2+\lambda)$, the effective pulse area is the same as that of the RZ sech pulse, so that for $\Omega/\sigma = \text{integer}$, the induced evolution is cyclic. I focus on cyclic evolution and specifically on $\Omega = \sigma$ and $\Omega = 2\sigma$, which will be referred to as 2π and 4π pulses respectively. A 2π (4π) pulse cycles the polarization vector from $|n\rangle$ toward $|E\rangle$ and back to $|n\rangle$ once (twice). Taking $\lambda = 0$ recovers the symmetric, unchirped sech pulses.

A cyclic evolution in general induces a phase to the state, i.e., the probability amplitude acquires a phase factor. Using the analytically solvable dynamics outlined above, I obtain the following expressions for the phases for 2π and 4π pulses respectively

$$\phi(2\pi) = 2 \arctan \left[\frac{2+\lambda}{2(1+\lambda)} \frac{\sigma}{\Delta} \right] \quad (1)$$

$$\phi(4\pi) = 2 \arctan \left[\frac{8(1+\lambda)(2+\lambda)\Delta/\sigma}{4(\Delta/\sigma)^2(1+\lambda)^2 - 3(2+\lambda)^2} \right] \quad (2)$$

In general, the pulses are defined through their pulse shape asymmetry and their chirp, but since the two are related for transitionless dynamics henceforth only the strength and asymmetry will be used to refer to each pulse. To examine the qualitative behavior of these pulses, I focus on three non trivial values for the asymmetry parameter, $\lambda = -3/4, -0.5, 1$ for which $z(t)$ can be inverted. The phase ϕ from Eqs. (1) and (2) is plotted against the detuning (in units of bandwidth) in Fig. 2, where one may notice that for a target phase ϕ , the phase is a slower varying function for the 4π set of pulses. Within that set, the curves with negative λ 's are even more slowly varying. In the limit $\lambda \rightarrow -1$ we get a horizontal straight line, which means that the phase is always -1 and 1 for 2 and 4π pulses respectively. This is somewhat reminiscent of adiabatic rapid passage, where chirped pulses invert population robustly in the presence of variations in detuning. Moreover, 4π pulses have larger detunings for the same phase, resulting in less real excitation of the leaky excited state.

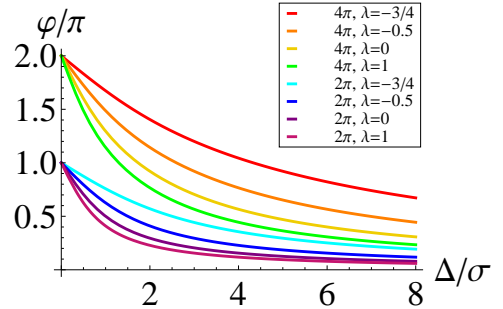


FIG. 2: (Color online) Phase (modulo 2π) as function of the detuning in units of pulse bandwidth for 4π and 2π pulses for various asymmetry parameters as shown in the legend.

In the present case, we expect the flatter pulses to be more robust against errors in the detuning. This statement is checked by calculating the fidelity of the phase gate implemented with each pulse as a function of the deviation from the ideal detuning. The fidelity is a measure of how close our evolution U is to the target evolution U_t , and is defined as $|\langle \psi | U^\dagger U_t | \psi \rangle|^2$, where the average is taken over all possible initial states $|\psi\rangle$. Indeed, calculations of the fidelity verify this expectation and quantify the performance of these gates, as can be seen from Fig. 3, where Δ_o is the ideal detuning for the target transition and is given in terms of the target phase and the pulse parameters σ, λ by inverting Eqs. 1 and 2. Even though in the case of chirped asymmetric pulses the deviation from the ideal detuning affects the probability of complete return to the ground state, these pulses are still more robust than their symmetric, unchirped coun-

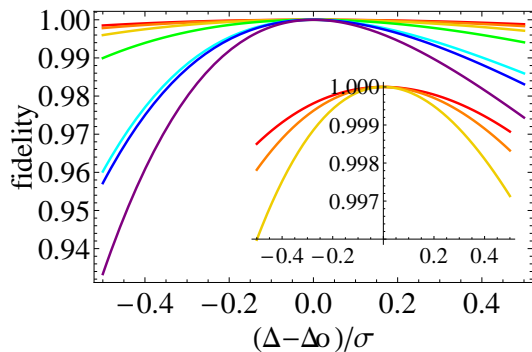


FIG. 3: (Color online) Fidelity of $\pi/2$ rotation as function of deviation from the ideal detuning Δ_0 for, from top to bottom, 4π $\lambda = -3/4$, 4π $\lambda = -0.5$, 4π $\lambda = 0$, 4π $\lambda = 1$, 2π $\lambda = -3/4$, 2π $\lambda = -0.5$, and 2π $\lambda = 0$. The pulse 2π $\lambda = 1$ is not included here as it performs worse than the 2π sech, as expected from the plots in Fig. 2. The inset shows the fidelities for only the three best performing 4π pulses in a scale where they can be distinguished.

terparts. The implication of this result is a highly desirable robustness against errors in the pulse frequency or uncertainty of system parameters. Furthermore, this insensitivity in the detuning in Fig. 3 tells us that we can implement high fidelity quantum gates in an inhomogeneous ensemble of systems by use of a single pulse. This is particularly important for human-made systems such as quantum dots, but it can also impact naturally occurring systems that interact with slightly different environments.

Another possible source of error can be the strength of the dipole of the transition. The various 4π pulses with different values of λ perform almost identically, while there is no significant difference within the 2π pulse subset either. However, the 4π pulses are overall superior to the 2π ones. This can be seen in the left panel of Fig. 4, where the fidelity is shown as a function of the phase for a 4π and for a 2π sech pulse with the dipole of the transition set to 1.05 times its target value. The superiority of the 4π pulse can be traced back to the larger detuning required for the same phase. Since the detuning is large, from a qualitative effective Rabi frequency argument, the relative importance of the coupling strength compared with the detuning is small for 4π pulses. However, for 2π pulses, where the control is almost resonant (and exactly resonant for a π rotation), the deviation from the ideal coupling strength will have a greater effect.

Now let's consider the case where state $|n\rangle$ is not an energy eigenstate, but instead a linear superposition of the two energy eigenstates of the qubit subspace. This is a common situation in quantum dot spin qubits, where there is an external magnetic field in the plane of the dot, while the laser propagates perpendicular to that along the growth axis and is circularly polarized. In that case, the light couples to the 'up' spin state along the growth

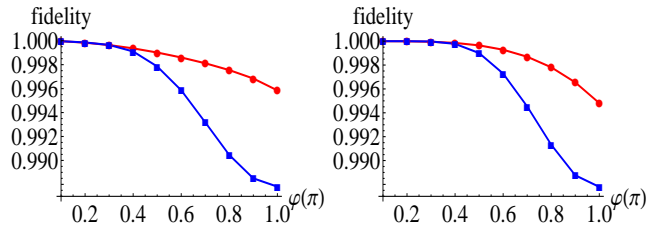


FIG. 4: (Color online) Left panel: Fidelity as function of the phase for 4π (red, circles) and 2π (blue, squares) pulses. The dipole of the transition is 5% higher than the ideal value. The 4π pulse is more robust to errors in the dipole. Right panel: Fidelity as function of the phase for 4π (red, circles) and 2π (blue, squares) pulses. The Zeeman splitting between the energy eigenstates of the qubit subspace is 10 times smaller than the bandwidth.

direction, which is not an energy eigenstate. The common assumption and experimental practice is to take the pulse duration to be much faster than the spin precession, so that the picture of Fig. 1 is valid (Otherwise the coupling between states $|n\rangle$ and $|\bar{n}\rangle$ should be taken into account, and the problem is no longer analytically solvable). It is therefore natural to ask what is the fidelity of the present pulses when the Zeeman splitting is not negligible compared to the pulse bandwidth. Again, the family of 4π pulses is found to perform better than their 2π counterparts [23], as can be seen in the right panel of Fig. 4. Since for the 4π pulses both the detuning and the pulse strength are larger than that of the 2π pulses, the relative importance of a larger Zeeman term is smaller in the former case, and hence the better performance.

Finally an important situation to examine is the case where there are other excited states that the laser couples to. In principle, these can be avoided by making the pulses temporally very long, i.e., very narrowband. This is generally not practical however, since long pulses excite the lossy auxiliary state $|E\rangle$ for longer times, increasing its chance to decay. Thus the compromise is to pick pulses that are narrowband compared to the energy difference between the target and unwanted transition, and broadband compared to the linewidth of the excited state. For such slower pulses, the fidelity is lowered predominately due to incoherent dynamics. This can be seen by calculating the purity of the qubit state after the passage of the pulse.

The purity is a measure of the incoherent dynamics and can be defined as $\text{Tr}(\rho^2)$, where ρ is the density matrix of the qubit. Clearly, for a system in a pure state, which can be described by a wave function, the purity is 1. It is instructive to look at the purity and fidelity of 2π versus 4π pulses. For this calculation, an additional excited state $|E'\rangle$ is included in the Hamiltonian (see caption of Fig. 5). First the bandwidths for which the fidelity is maximized are found numerically for each of the 2π and 4π pulses (this happens for different bandwidths for each

case), and the corresponding purity is calculated. The low values of the latter, as shown in the right panel of Fig. 5, indicate that indeed most of the fidelity loss is due to incoherent dynamics.

It is particularly interesting that while the maximal purity and fidelity coincide at a certain value of σ for the 2π pulse, they occur at different values of σ for the 4π pulse. Moreover, for the latter the maximal purity is very high, much larger than that of the 2π pulse, at a bandwidth that is comparable to the splitting from the unwanted transition. What this tells us is that the loss of fidelity comes almost exclusively from unintended dynamics, i.e., that crucially the population is returned to the qubit subspace once the pulse has passed. This surprising result is important because it means that there exists a fast high fidelity phase gate corresponding to this pulse. So essentially we have unitary but unknown dynamics. This observation opens up the key question of how to explicitly determine the actual, almost unitary evolution corresponding to the fast, high purity pulse. The analytically solvable dynamics presented here, in combination with approximate methods such as split-operator techniques or other expansions, offer a promising starting point for determining the evolution operator when additional excited state dynamics are involved. This pursuit would advance the design of quantum controls for a variety of realistic systems.

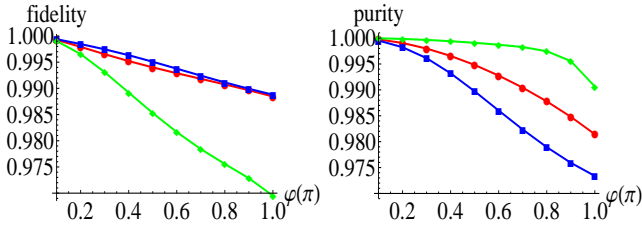


FIG. 5: (Color online) Gate performance in the presence of additional excited state $|E'\rangle$ and decay. The transition $|n\rangle \rightarrow |E'\rangle$ is taken to be 0.2 meV higher in frequency from $|n\rangle \rightarrow |E\rangle$ and to have half the coupling strength (qualitatively similar results are obtained for both higher and lower coupling strengths). The decay rates are set to $0.8\mu\text{eV}$. Left panel: Fidelity as function of the phase for 4π pulse with $\sigma = 0.03\text{meV}$ (red, circles) and 2π pulse with $\sigma = 0.06\text{meV}$ (blue, squares). The green (diamonds) curve corresponds to the fidelity of a fast 4π sech pulse with $\sigma = 0.2\text{meV}$. Right panel: Purity as function of the phase for 4π (red, circles) and 2π (blue, squares) pulses with the maximal fidelity, see left panel. The green (diamonds) curve is the maximal purity for a 4π sech pulse. Note that the parameters used here are taken from quantum dot spin qubits, but are consistent with atomic/ionic qubits since the energy scales in those systems are all about an order of magnitude smaller.

In conclusion, I have shown that high fidelity phase gates can be achieved in realistic systems by use of a family of analytically solvable pulses that may have asymmetric temporal shapes and frequency modulation. The

superior quality of these controls, as quantified by the fidelity, stems from their robustness against imperfections. Moreover, the relatively simple analytical expressions derived here greatly facilitate the design of experimental implementation of phase gates. The latter are important as they suffice for universal quantum logic. In addition, this work opens up the possibility of incorporating off-resonant states into the control schemes, thus allowing for simultaneously fast and accurate control, an attractive feature when limited coherence times are available.

This work was supported by LPS/NSA and in part by ONR. I thank Edwin Barnes for fruitful discussions.

-
- [1] M. A. Nielsen and I. L. Chuang, Quantum Computation and Quantum Information (Cambridge Univ. Press).
 - [2] D. Press, T. D. Ladd, B. Zhang, and Y. Yamamoto, Nature **456**, 218 (2008).
 - [3] A. Greilich, S. E. Economou, S. Spatzek, D. R. Yakovlev, D. Reuter, A. D. Wieck, T. L. Reinecke, and M. Bayer, Nature Physics **5**, 262 (2009).
 - [4] D. Kim, S. G. Carter, A. Greilich, A. S. Bracker and D. Gammon, Nature Physics **7**, 223 (2011).
 - [5] T. M. Godden, J. H. Quilter, A. J. Ramsay, Y. Wu, P. Brereton, S. J. Boyle, I. J. Luxmoore, J. Puebla-Nunez, A. M. Fox, and M. S. Skolnick, Phys. Rev. Lett. **108**, 017402 (2012).
 - [6] C. Phelps, T. Sweeney, R. T. Cox, and H. Wang, Phys. Rev. Lett. **102**, 237402 (2009); T. M. Sweeney, C. Phelps, and H. Wang, Phys. Rev. B **84**, 075321 (2011).
 - [7] W. C. Campbell, J. Mizrahi, Q. Quraishi, C. Senko, D. Hayes, D. Hucul, D. N. Matsukevich, P. Maunz, and C. Monroe, Phys. Rev. Lett. **105**, 090502 (2010).
 - [8] M. Saffman, T. G. Walker, and K. Molmer, Rev. Mod. Phys. **82**, 2313 (2010).
 - [9] B. B. Buckley, G. D. Fuchs, L. C. Bassett and D. D. Awschalom, Science **330**, 1212 (2010).
 - [10] L. DiCarlo, J. M. Chow, J. M. Gambetta, L. S. Bishop, B. R. Johnson, D. I. Schuster, J. Majer, A. Blais, L. Frunzio, S. M. Girvin, and R. J. Schoelkopf, Nature **460**, 240 (2009).
 - [11] E. D. Kim, K. Truex, X. Xu, B. Sun, D. G. Steel, A. S. Bracker, D. Gammon, and L. J. Sham, Phys. Rev. Lett. **104**, 167401 (2010).
 - [12] E. Poem, O. Kenneth, Y. Kodriano, Y. Benny, S. Khatsevich, J. E. Avron, and D. Gershoni, Phys. Rev. Lett. **107**, 087401 (2011).
 - [13] C. Monroe, D. M. Meekhof, B.E. King, W. M. Itano, and D.J. Wineland, Phys. Rev. Lett. **75**, 4714 (1995).
 - [14] J. J. L. Morton, A. M. Tyryshkin, A. Ardavan, S. C. Benjamin, K. Porfyakis, S. A. Lyon and G. A. D. Briggs, Nature Physics **2**, 40 (2005).
 - [15] J. R. Schrieffer and P. A. Wolff, Phys. Rev. **149**, 491 (1966).
 - [16] N. Rosen and C. Zener, Phys. Rev. **40**, 502 (1932).
 - [17] S. E. Economou, L. J. Sham, Y. Wu, and D. G. Steel, Phys. Rev. B **74**, 205415 (2006); S. E. Economou and T. L. Reinecke, Phys. Rev. Lett. **99**, 217401 (2007).
 - [18] Y. Wu, I. M. Piper, M. Ediger, P. Brereton, E. R. Schmidgall, P. R. Eastham, M. Hugues, M. Hopkinson,

- and R. T. Phillips, Phys. Rev. Lett. **106**, 067401 (2011).
- [19] C.-M. Simon, T. Belhadj, B. Chatel, T. Amand, P. Renucci, A. Lemaitre, O. Krebs, P. A. Dalgarno, R. J. Warburton, X. Marie, and B. Urbaszek, Phys. Rev. Lett. **106**, 166801 (2011).
- [20] S. McCall and E. Hahn, Phys. Rev. **183** (1969).
- [21] A. Bambini and P. R. Berman, Phys. Rev. A **23**, 2496 (1981).
- [22] F. T. Hioe, Phys. Rev. A **30**, 2100 (1984); J. Zakrzewski, Phys. Rev. A **32**, 3748 (1985); E. J. Robinson, Phys. Rev. A **31**, 3986 (1985).
- [23] P. Pei, F-Y Zhang, C. Li, and H-S Song, J. Phys. B: At. Mol. Opt. Phys. **43**, 125504 (2010).